Chapter 9
Vacuum Frictionless Mechanisms Based on the Principle of Controlled Elastic Deformation

The idea of these mechanisms was born between 1970–1980 in the former USSR and it was realized by Professor A.T. Alexandrova. The group of Professor Alexandrova designed and manufactured different vacuum manipulators, vacuum drives, vacuum rotary-motion and linear-motion feedthroughs, gates and valves based on the principle of controlled elastic deformation. This work was pioneer in the field of vacuum technique and technology.

In many cases the applicability of traditional gears, ball bearings and friction couples is limited in vacuum because of gas tribodesorption, wear of contacting surfaces, limited service life of friction couple (see Chapters 3 and 7). The solution of these problems can be found by controlling friction, wear and gas tribodesorption vacuum mechanisms as well as by use of frictionless mechanisms based on the principle of controlled elastic deformation.

Not all vacuum mechanisms could be realized using controlled elastic deformation of vacuum mechanisms. Nevertheless, in many cases, for example for fast-acting vacuum manipulators, transporting systems, precise positioning systems, bodiless vacuum gates and valves, and other small mechanisms, the use of controlled elastic deformation of vacuum mechanisms is very promising because of compactness, low weight and absence of interfacial friction.

The elemental basis of vacuum mechanisms without friction couples consists of various hermetic driving tube elements of different configurations (as shown in Figure 9.1). These elements can be deformed by supplying compressed gas or liquid inside the tube elements under controlled pressure.

The radius of curvature of the center axis of hermetic driving elements of different configurations can be varied according to different principles of variation. In case of non-finite number of elements (Figure 9.1a–g) it essentially influences the trajectory of free end of the driving element. The cross-section geometric shape of hermetic driving elements can be realized in the following variants shown in Figure 9.1j: elliptic, rhombic, concavo-concave and others. The geometric shape of the

E.A. Deulin et al., *Mechanics and Physics of Precise Vacuum Mechanisms*,
Fluid Mechanics and Its Applications 91, DOI 10.1007/978-90-481-2520-3_9,

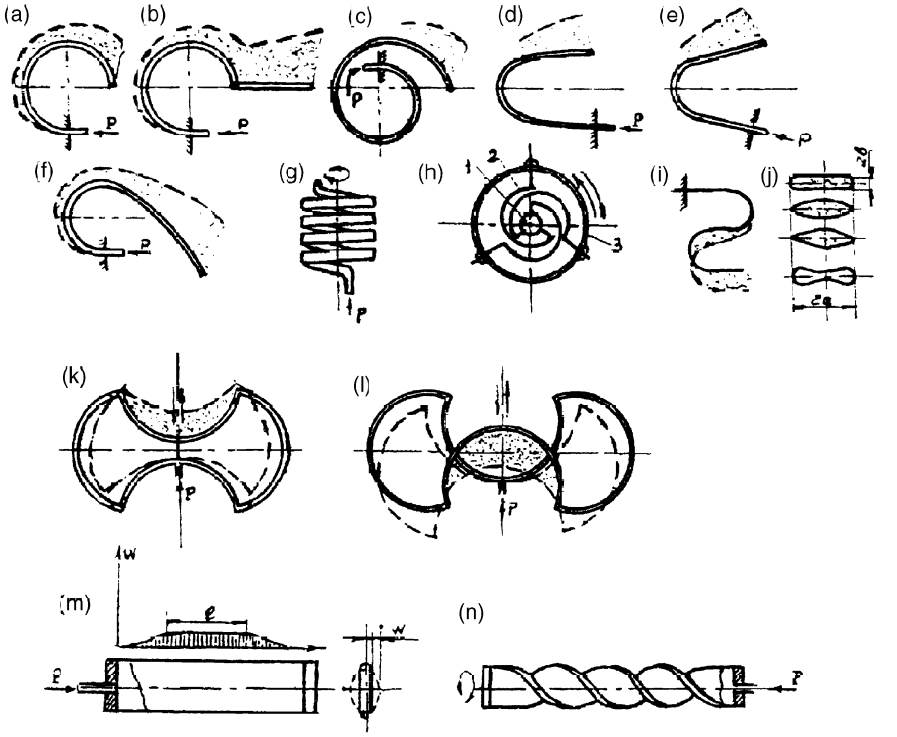

Fig. 9.1 Variants of the drives schemes based on controlled elastic deformation principle.

cross-section of hermetic driving element determines the following parameters of drives: sensitivity, maximum displacement and loading capability of the drive.

The simplest and the most technological types of design are the drives with constant radius of curvature (Figures 9.1a–b). The displacement range of these elements can be multiplied by their combination with layers.

Special drives with shape of Archimedes's spiral Figure 9.1c, parabola Figure 9.1d, sinusoid Figure 9.1e and cycloid Figure 9.1f are designed to realize displacement on specific trajectories.

Multi-turn can realize circular displacement for various angles which depend on the total number of coils. Circular displacement can be realized also using three free-ended drives (position 2 in Figure 9.1h). These elements are connected by one side to the supply line of gas or liquid by the collector 1, while another side is connected to the outer ring 3. The advantage of this scheme is the possibility of every drive 2 to ensure isolated radial output. The drives of closed contour (Figures 9.1k–l) are designed for linear displacement. The drives formed with linear axis are designed for precise linear displacement (see Figure 9.1m) and for precise angular (circular) displacements (see Figure 9.1n).

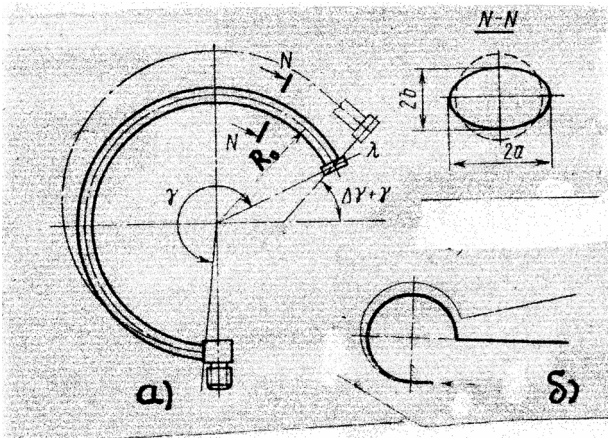

Fig. 9.2 Calculation scheme of the drive based on controlled elastic deformation principle which corresponds to open-ended contour.

New manipulators and mechanisms with a large number of degrees of freedom which can realize complex trajectories can be developed by combination of some of these driving elements of controlled elastic deformation either between them or with metal bellows.

Geometrical parameters of elastically deformed drives of free-ended type contour are shown in Figures 9.2a–b. The transference λ of the free end of this drive and developed force of this drive are determined using an energy method (Roots Method). In result of a second redevelopment of the Roots Method the following equations were obtained for simple engineering calculation:

$$\lambda = \frac{PR_0^3(D_6 + D_7\nu)}{Eah(D_3 + D_4\nu + D\nu^2)}\sqrt{(\gamma - \sin\gamma)^2 + (1 - \cos\gamma)^2}, \tag{9.1}$$

$$Q_\tau = 4Pa^2\frac{D_6 + D_7\nu}{D_0 + D_1\nu + D_2\nu^2}\frac{2(\gamma - \sin\gamma)}{3\gamma - 4\sin\gamma + 1/2\sin 2\gamma}, \tag{9.2}$$

$$Q_{r\tau} = 4Pa^2\frac{D_6 + D_7\nu}{D_0 + D_1\nu + D_2\nu^2}\frac{4(1 - \cos\gamma)}{2\gamma - \sin 2\gamma}, \tag{9.3}$$

where E is the modulus of elasticity of the drive material; Q_τ and Q_r are the tangential and radial tractive forces, respectively; R_0 is the initial radius of curvature of the central axis of the driving; h is the wall thickness of the element; a, b are the large and small axes of cross-section; $D_0 \ldots D_7$ are the coefficients which depend on the shape of normal cross-section and ratio of axes (see Table 9.1). The ratio of the large to small axes $a/b = k$; ν is the non-dimensional parameter which can be calculated from

$$\nu = \frac{R_0^2h^2}{12(1 - \mu^2)a^4}, \tag{9.4}$$

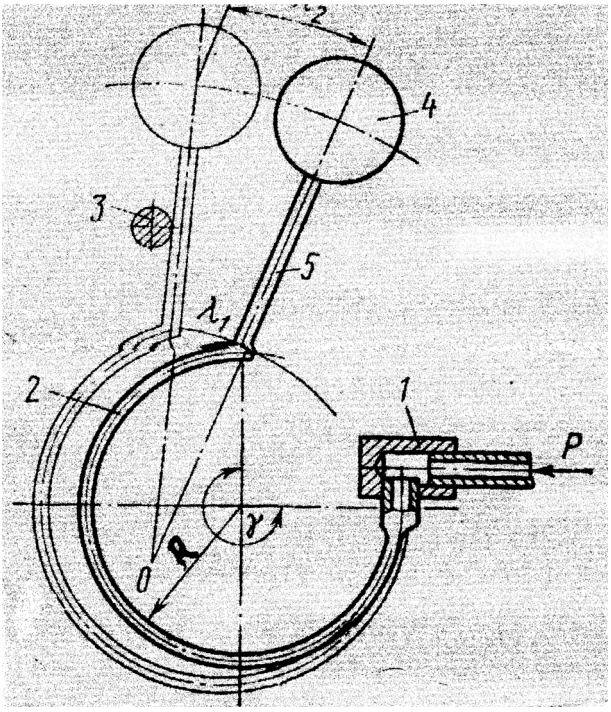

Fig. 9.3 Scheme of screening device.

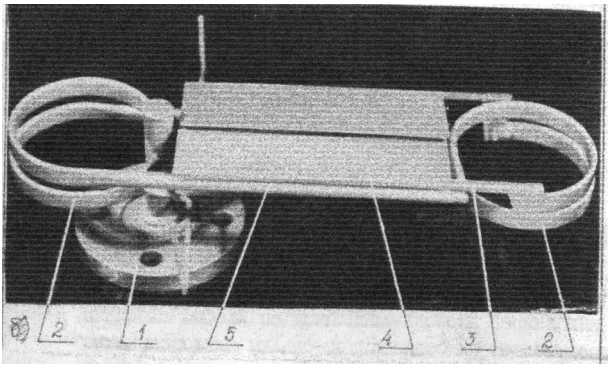

Fig. 9.4 Scheme of two-folding screening device.

where μ is the Poisson ratio.

One of the simplest devices based on controlled elastic deformation is the screening shield. Figure 9.3 shows the scheme of a screening shield which consists of the connecting pipe 1, the drive 2, the support 3 which limits the position of the screen 4, and the lever 5. Figure 9.4 shows a bivalve (butterfly-type) screening shield. The

Table 9.1 Table of coefficients.

View of cross-section	Ratio of large to small axes $a/b = k$	Values of coefficient for $h/b < 0.3$							
		D_0	D_1	D_2	D_3	D_4	D_5	D_6	D_7
Oval plane	2	34.5	33122	595992	0.7	1400	133010	9	9100
	3	78	65350	1295773	0.8	1503	133676	18	14256
	4	89	73692	1562383	0.6	1053	92410	17	12620
	5	89	73780	1643135	0.4	718	62904	14	10266
	6	85	71528	1654052	0.3	504	44302	12	8340
Rhombic $r = b/4$	1	91	75747	1854078	0.1	240	88603	16	11871
	2	71	62061	1613217	0.055	118	43063	9.5	7623
	3	62	55595	1495687	0.03	71	25540	7.0	5571
Rhombic $r = b/5$	1	86	72721	1816548	0.08	195	83185	14.5	11138
	2	67	59548	1576173	0.04	95	40173	9	7152
	3	58	53466	1461614	0.02	57	23777	6	5240

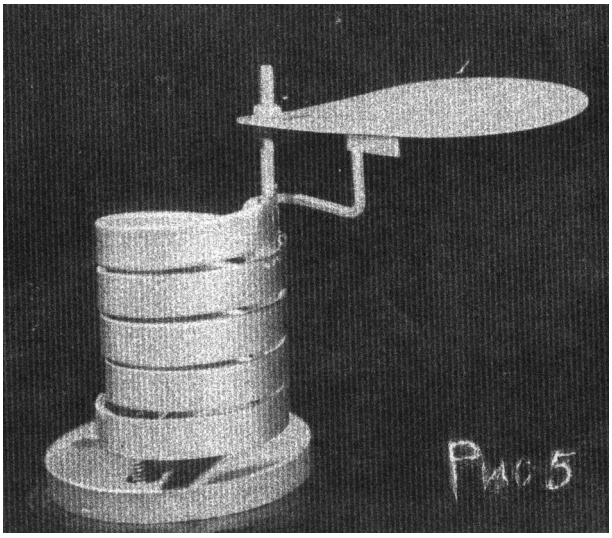

Fig. 9.5 Screening device with multi coil drive.

lever 5 moves parallel to the screen 4. The second pair of drives can be attached to the device in order to perform displacement in opposite directions (Figure 9.4). When the angular transference should be increased, a multi-turn drive can be used (Figure 9.5).

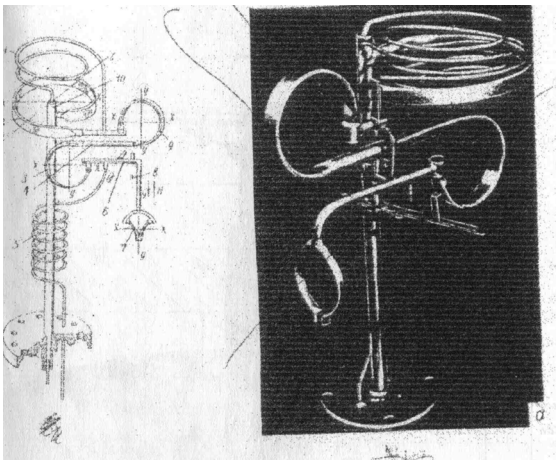

Fig. 9.6a Manipulator: (left) scheme, (right) general view.

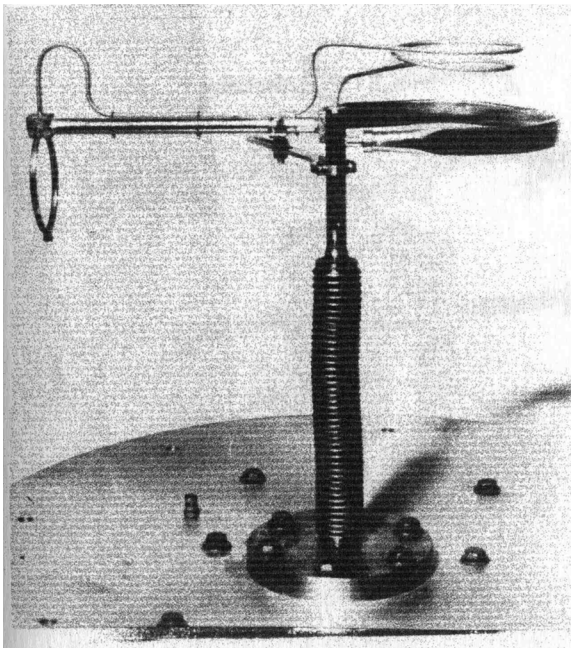

Fig. 9.6b The manipulator based on unclosed contour for usage in multifunctional devices of vacuum mechanics.

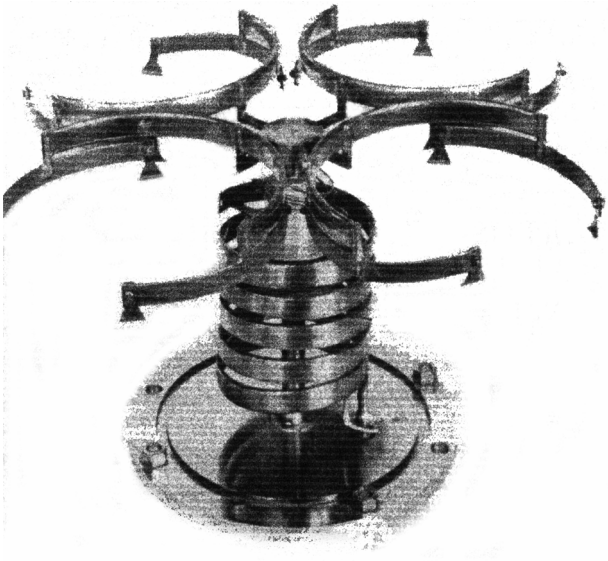

Fig. 9.7 Four position transfer manipulator of wafers.

Figure 9.6 shows an example of a drive of unclosed type which can be used for development of various vacuum mechanisms. This drive has three degrees of freedom.

The clamp 7 can turn around a vertical axis by driving element 2 and can be displaced in vertical direction by the elements 3 and 9. These elements are made of hermetically sealed tubes which allows us to extend the displacement range.

The sample capture is realized using clamp 7, which consists of a collector and two elastically deformed driving elements. Each motion is realized by the pressure control separately in each driving element through the tubes 10, 1 and 5. The tubes 1 and 5 contain spiral compensators. After angular transference the clamp position is fixed by supports 8.

A positioning manipulator for transfer of waters and other flat samples with diameter up to 200 mm was designed. The maximum angular displacement of this manipulator exceeds 90 degrees. The manipulator is based on a multi-turn drive which performs a near-circular motion (see Figure 9.7).

The manipulator is combined of four driving elements. Also there is a bellow pneumodrive for vertical displacement of the clamp (Figures 9.7 and 9.8).

The total angular displacement $\Delta_{\gamma\Sigma}$ of the free end of the drive is proportional to the number of coils and can be calculated from the following equation:

$$\Delta_{\gamma\Sigma} = n\gamma \frac{PR_0^2(D_6 + D_7\nu)}{Eah(D_3 + D_4\nu + D_5\nu^2)},$$

where γ is the central angle of the drive.

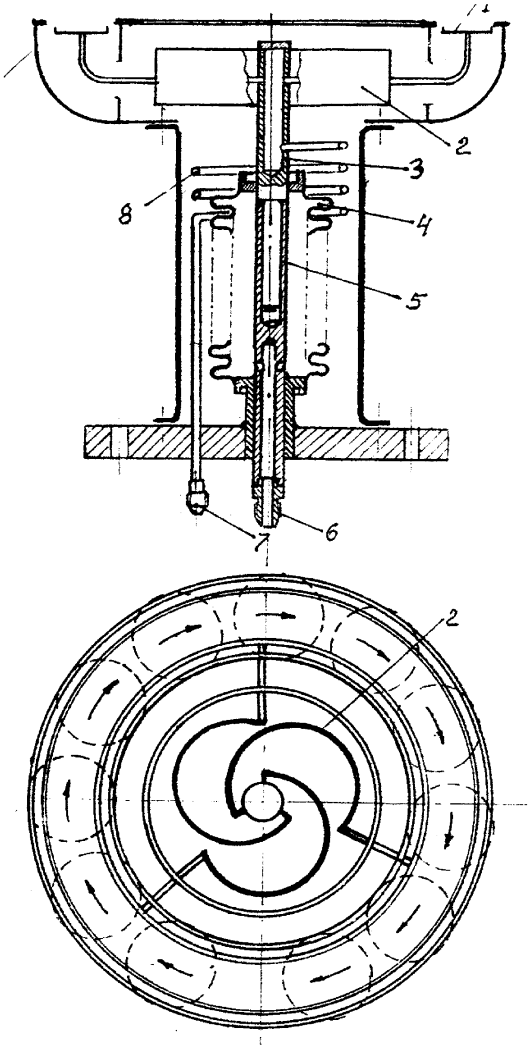

Fig. 9.8 Manipulator for circular transporation of wafers.

The turning drives shown in Figure 9.1b can be used in transporting systems of discrete action of multiposition vacuum equipment.

The scheme of a transporting device for sample displacement is shown in Figure 9.8. The drive of the device is a drive of discrete circular displacement 2 and consists of a bearing ring 1, guides 9 and bellows drive 4 of vertical transference. Bearing ring 1 moves in circular and in vertical directions and realizes the following operations: “taking – transferring – laying down”. Gas supply of the bellows drive

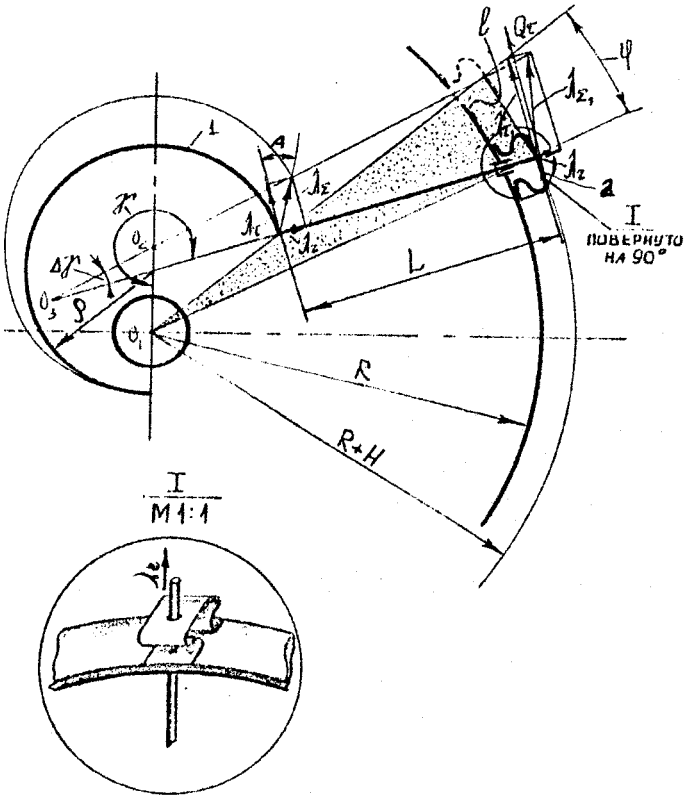

Fig. 9.9 Scheme for determination of the angular circular displacement.

is realized through the connecting pipe 7, and the tube with compensator 8 and the tube collector 3.

The scheme for determination of angular and circular displacement is shown in Figure 9.9. The circular errors, Q_1, Q_2 and Q_3, correspond to center of rotating device, initial center and momentary center of the curve of elastically deformed drive.

As follows from Figure 9.9 the angle of the ring rotation can be determined by

$$\varphi = 2 \arcsin \frac{l}{2(R+H)},$$

where R is the radius of outer ring of the drive; H is the height of the compensator. For engineering calculation it can be assumed that that

$$l = \lambda \tau_1,$$

where $\lambda\tau_1$ is the tangential component of the lever of length L. The value $\lambda\tau_1$ can be determined from:

$$\lambda\tau_1 = \frac{L\sin\Delta\gamma + \lambda_\Sigma \sin\Delta\gamma + \lambda_\Sigma \cos(A+\Delta\gamma)}{\lambda_\Sigma \cos(A+\Delta\gamma) + \lambda_r \sin\Delta\gamma}\lambda_\tau,$$

where $\Delta\gamma$ is the variation of the central angle γ of the driving tube; λ_τ, λ_r are the tangential and radial components of displacement which is formed by the free end of the tube element: λ_Σ is the total displacement of the free end of the tube element; A is the angle between the vector of the total displacement λ_Σ and the tangent vector of the central axis of the tube element. The values of the parameters λ_τ, λ_r and λ_Σ may be determined from the following equations:

$$\begin{aligned}
\lambda_\tau &= \frac{\Delta\gamma}{\gamma}R(\gamma - \sin\gamma),\\
\lambda_r &= \frac{\Delta\gamma}{\gamma}P(1-\cos\gamma),\\
\lambda_\Sigma &= \sqrt{\gamma_\tau^2 + \lambda_r^2},\\
A &= \arctan\frac{(1-\cos\gamma)}{(1-\sin\gamma)}.
\end{aligned}$$

Torque of the ring M has three components of loading force. These components coincide with the direction of tangential component of the torque:

$$M = 3Q\tau R.$$

The value Q_τ can be determined from Equation (9.2) taking into account the transmission ratio of the lever L. For the termination of the motion in radial direction λ_r, the spring compensators (pos. 2) are used. These compensators are fixed to the end of elastically deformed elements. The rigidity of these compensators in circle direction must be high enough for torque transmission.

The drives with a closed contour are the simplest and most useful from a technological point of view (see Figure 9.1). In the drives of these types there are four hermetic curved tubes of constant radius of curvature. The tubes are connected one to another and form a plane contour.

The scheme of the drive is shown in Figure 9.10. The resulting displacement in central point B along axis Y is determined by the total displacement deformation of the total perimeter of contour S. In the general case the resulting displacement can be determined by the integral:

$$\lambda_B = \int \frac{\phi(\varphi)}{\rho(\varphi)}M_1(\varphi)dS,$$

where $M_1(\varphi)$ is the bending moment in arbitrary cross-section of the tube as a function of unity force in the direction of specific displacement; $\psi(\varphi)$ is the angle of tor-

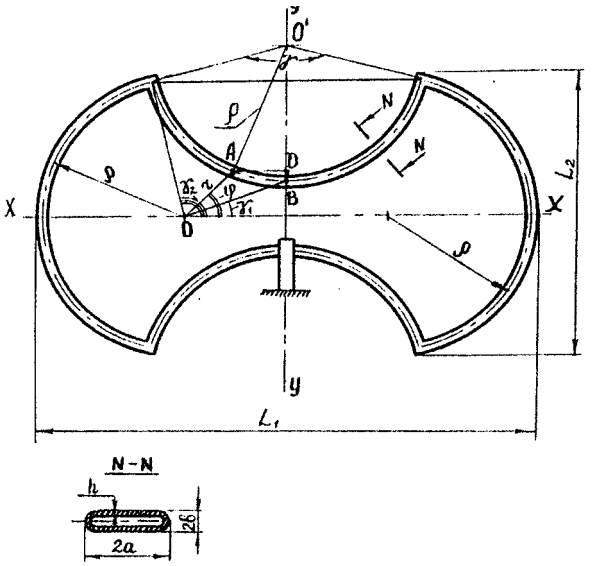

Fig. 9.10 The scheme for calculation of the drive of the closed type.

Table 9.2 The angle parameters (in degrees).

γ	90	120	150	210	240	270
γ_1	90	45	17.6	–13.4	–24.9	–35.3
γ_2	135	120	105	75	60	45

sion in the arbitrary cross-section; $\rho(\varphi)$ is the curve radius of contour element. The geometry parameters of elastic line of the contour depends on the angles γ, γ_1, γ_2:

$$\gamma_2 = \pi - \gamma/2.$$

The angle γ_1 is determined from the triangle OBC:

$$\gamma_1 = \arctan \frac{\sin \gamma/2 + \cos \gamma/2 - 1}{\sin \gamma/2 - \cos \gamma/2}$$

Table 9.2 shows several values of the angles. Figure 9.11 shows the contour form for two cases:

$$\gamma \leq 180^\circ \quad \text{and} \quad \gamma > 180^\circ.$$

The drive generate a force in the direction of the displacement which can be expressed in general form as

$$Q = \frac{E K I_a \int_S \frac{\phi(\varphi)}{\rho\varphi}[r(\gamma_1)\cos\gamma_1 - r\varphi\cos\varphi]dS}{1 - \mu^2 \int_S [r(\gamma_1)\cos\gamma_1 - r(\varphi)\cos\varphi]^2 dS},$$

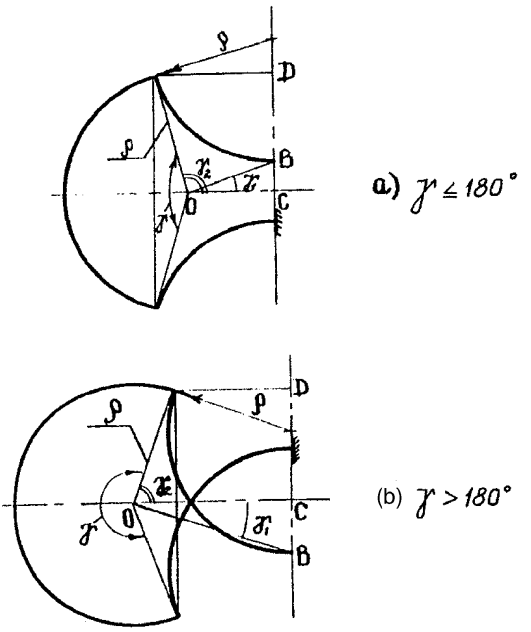

Fig. 9.11 Drives contours with different L: (a) $\gamma \leq 180°$; (b) $\gamma > 180°$.

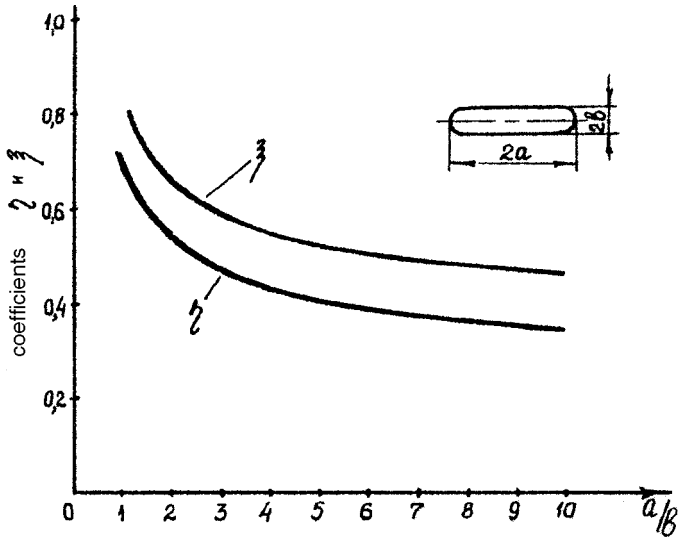

Fig. 9.12 The values of coefficients η, ξ for plane-oval cross-section.

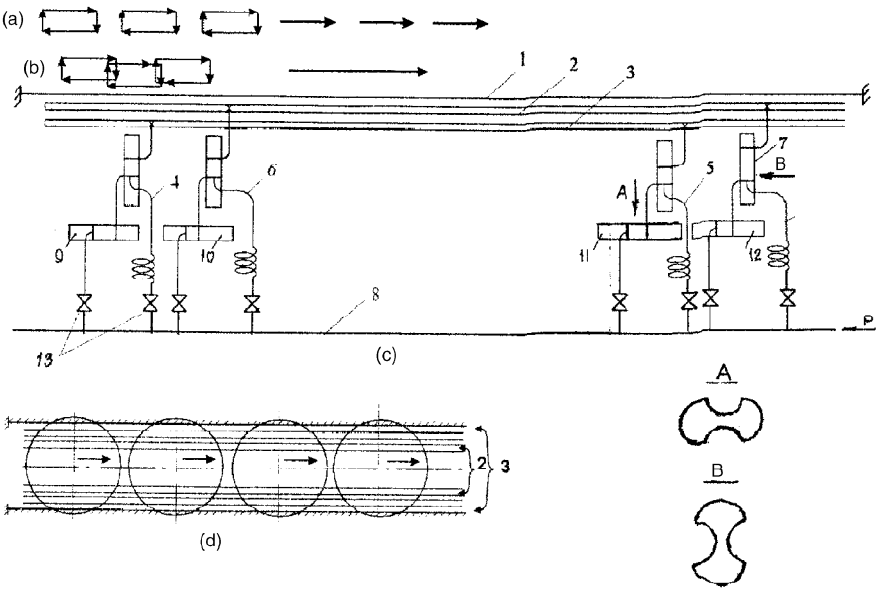

Fig. 9.13 Scheme of transporting system.

where r is a parameter shown in Figure 9.11; E is the modulus of elasticity of the drive elements material; μ is the Poisson coefficient; I_a is the moment of inertia of cross-section in respect to the large axis; K is the coefficient depending on the deformation of the cross-section element and curvature of contour of the central axis.

For the most commonly used plane-oval cross-section we have the following equation:

$$I_a = 4_{B^3h}(a/b - 1 + \pi/4),$$
$$K = 1 - \eta/(\xi + \chi^2).$$

where χ is the main parameter of the element $\chi = \rho h/a^2$; η, ξ are the coefficients which depend on the shape and the axis ratio of the normal section and the cross-section. Coefficients η, ξ for plane-oval cross-section are shown in Figure 9.12.

The drives of loop-controlled contour have high rigidity. These drives have enhanced dynamic parameters and a high damping factor of damped oscillation. They can be used successfully for linear transportation of samples. However, the direction of displacement trajectories depends on the geometry of the drive axis in space.

Figure 9.13 shows a variant of a transportation system which is designed on the basis of a loop-controlled drive contour. This drive allows intermittent (discrete) and streaming modes of operation. In the first case (Figure 9.13a) the drive realizes the operation mode "taking – transferring – laying down" and in the second case

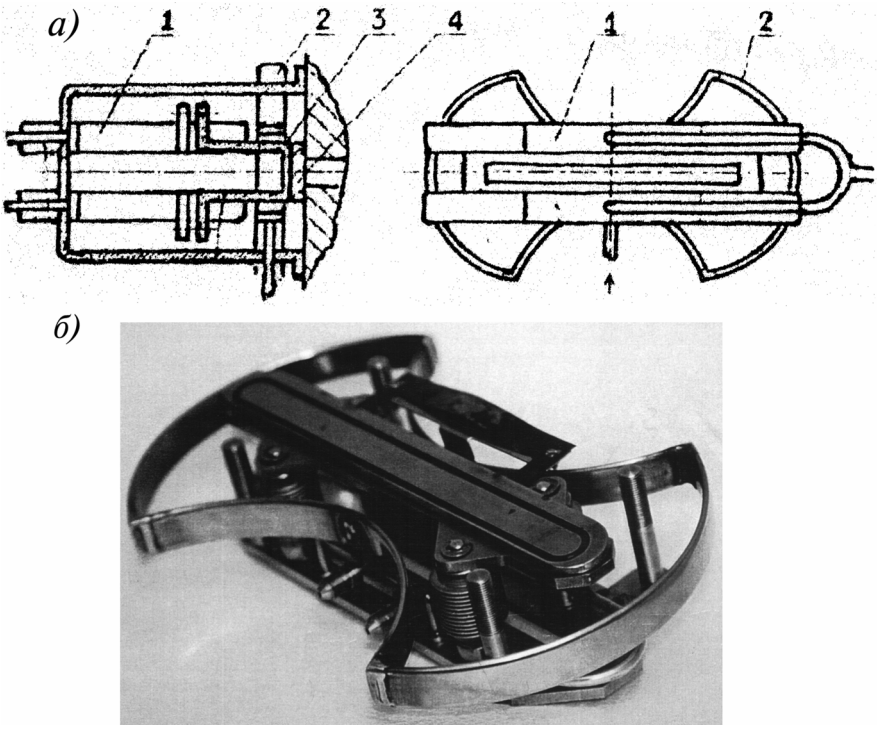

Fig. 9.14 Bodiless vacuum gate of slit type: (a) scheme of design, (b) general view.

(Figure 9.13b) the drive realizes the operation "taking – transferring". In the last case the displacement can be realized on required distance because of superposition of driving impulses. In the case of the intermittent mode of operation the drives 4, 5, 9, 11 are used; in the case of the streaming mode of operation the drives 4 to 7 and 9 to 12 are used. The system consists of two pairs of mobile guides 2 and 3 placed along a static guide 1.

A vertical displacement of movable guides 2 and 3 is realized using the drives 4, 5, 6, 7; the horizontal transference is realized by the drives 9, 10, 11, 12. Compressed gas or liquid are supplied from the common collector 8. Sequences of switching of electromagnetic valves 13 is controlled by a program according to the required regime of the operation.

The speed of transference can reach 100 mm/s in a streaming mode of operation. By using liquid the 2 or 3 coordinate precise simple drive with loop control can be developed. The drives were used for aperture diaphragms in electron beam installations and other electronic technological equipment. Figure 9.14 shows the scheme of a loop-controlled contour of the drive of bodiless vacuum gate. This type of vacuum gate can be used for isolation of a vacuum system sealing under small pressure difference.

In a vacuum gate of this type, two drives 1 create the sealing load through the clamping cramp 3. The drive 2 through the flexible element rises sealing strap 4 in vertical direction and opens the slit hole. The considered drives can be manufactured from thin-wall tubes with wall thickness 0.15–0.2 mm. These thin-wall tubes are made by a solid-drawn method and then the required normal cross-section and curve radius of central axis are obtained by deformation. Steel used for manufacturing of the driving tube elements have good elastically durability, vacuum technological and processing characteristics. The following steels can be recommended for manufacturing of thin-wall driving tubes: 36NiCrTiAl, 2Cr13, 08Cr18Ni10Ti.